Proc. of the 9th Intl. Conf. of Asian Society for Precision Engg. and Nanotechnology (ASPEN 2022)
15–18 November 2022, Singapore. Edited by Nai Mui Ling Sharon and A. Senthil Kumar
doi://10.3850/978-981-18-6021-8_OR-02-0100

Design of a Cable-Driven Continuum Manipulator for Applications in Confined Spaces at Elevated Heights

Landong Martua[1] and Mustafa Shabbir Kurbanhusen[1,#]
1 Engineering Cluster, Singapore Institute of Technology, 10 Dover Drive, 138683, Singapore
Corresponding Author / Email: Mustafa.Shabbir@Singaporetech.edu.sg, TEL: +65 6592 2190

KEYWORDS: Cable-driven robots, Continuum robots

Inspecting confined spaces at elevated locations such as pot bearing housings in railway viaducts are challenging. Elevated work platforms are typically used to hoist people and equipment to conduct the inspection manually, which are often time-consuming, laborious and at times, physically inaccessible. A unique combination of a tethered aerial drone, integrated with a lightweight manipulator is proposed to overcome this challenge, where the lightweight manipulator is based on a cable-driven concept with a continuous backbone design. The cable-driven concept allows the manipulator to be lightweight enough to be mounted onto the aerial drone as the driving cables on the manipulator are connected via a tethering line to the cable winching units that are housed on the ground. The continuous backbone design, on the other hand, offers selective flexibility and rigidity in different planes to maneuver in confined complex spaces. In this paper, a four degrees-of-freedom cable-driven manipulator is presented, along with a continuous backbone design, inspired by the flexible ruler, which offers high bending stiffness in the vertical direction to minimize downward deflection of the manipulator, with low bending stiffness in the horizontal direction to maximize the flexibility of maneuvering in confined and complex spaces. The kinematics model is derived using the modified D-H method, with a constant curvature compensation factor, followed by FEA studies, before developing the actual prototype. Experimental validations on the accuracy of the derived kinematic model and the FEA simulations were found to be approximately 95%. The resulting prototype is a metre long lightweight cable-driven manipulator with a 50mm cross-sectional diameter, weighing less than 650 grammes, and driven by eight actuating cables to achieve the four degrees-of -freedom motion required for the inspection task in confined spaces at elevated locations.

NOMENCLATURE

d1 = axial translation of module 1
θ = yaw angle of each module
n = number of spacer disk of each module
s = backbone length of each module
X = shortest distance from start to end of the backbone
T= Homogenous transformation matrix

1. Introduction

Continuous monitoring and maintenance of infrastructure and building structures in rail transport such as pot bearing housings in railway viaducts (see Fig. 1), are critical to minimize any breakdown in critical services. Currently, significant portion of such monitoring work located at elevated locations are carried out using aerial work platform (AWP). An AWP is a mechanical device that is used to hoist and provide temporary access to people and equipment to reach inaccessible areas at heights. It is also known as an elevated work platform (EWP), bucket truck or cherry picket [1]. The use of AWP is often time-consuming, laborious and at times, physically inaccessible, which presents a gap to be addressed to enhance the productivity in conducting such maintenance tasks.

Fig. 1 Pot bearing housings in railway viaducts

In the following sections, this paper will detail the design of a lightweight cable-driven continuum manipulator, including the derivation of its kinematics model using the modified D-H method and incorporating a constant curvature compensation factor, followed by FEA studies, before comparing the results with the actual prototype.

2. Design Overview of The Cable-Driven Continuum Manipulator

In order to meet the requirements of inspecting confined spaces at elevated locations, a unique combination of an aerial drone, integrated with a lightweight cable-driven continuum manipulator was proposed. As shown in Fig. 2, the cable-driven continuum manipulator system comprised of the continuum manipulator attached to the aerial drone, and the actuation transmitted to a mobile actuation unit via a tethering line. The actuation unit consisted of a motor controller, motor drivers and graphical user interface that could be programed to automatically control the manipulator maneuvers inside a confined space with a known geometry, or control manually by the operator via a joystick. Transmission of the mechanical force from the actuation unit to the manipulator was via tethering line. It was designed to be easily detachable from the actuation unit with a fast release mechanism. The lightweight cable-driven manipulator with a linear guide rail could be place at top, mid or bottom of the drone. With the fast release mechanism, the manipulator and tethering line could also be detached from the drone after operation for ease in transportation.

As shown in Fig. 3, the continuum manipulator consisted of four modules, each having one DOF, and combining to a total of four DOF manipulator, thereby allowing it to generate motion in both axial and longitudinal directions. The continuous backbone design was inspired by the flexible ruler, which offered high bending stiffness in the vertical direction to minimize downward deflection of the manipulator, and low bending stiffness in the horizontal direction to maximize the flexibility of maneuvering in confined and complex spaces.

As required by the application scenario, the manipulator must be able to perform inspection of confined spaces at elevated locations such as pot bearing housings in railway viaducts as shown in Fig. 1, and the end-effector must be able to reach back of the pot bearing for inspection. With the typical outer diameter of the pot bearing being 50mm, the manipulator required a length of atleast a metre in order to reach the back of the pot bearing. As such, the metre long manipulator was divided in four modules, with Module 1 providing the 1-DOF linear translational motion into the crevice once the aerial drone had docked on to the viaduct gap. It consisted of a combination of a lightweight T-type 12mm linear guide rail with a length of 1m and T-type miniature guide carriage TW-04 from Igus®. As for Modules 2, 3 and 4, each provided a 1-DOF yaw orientation and having lengths of 300mm, 350mm and 350mm respectively (see Fig. 3). Each module would be controlled by two actuation cables. The continuum backbone employed a flexible ruler-like structure, which has low bending stiffness in horizontal direction and high bending stiffness in vertical direction. As a result of such configuration, the downward deflection was minimized and the number of actuation cable was reduced to two for each yaw module i.e., Modules 2, 3 and 4. This resulted in a total of 8 actuating cables for the entire 4-DOF manipulator. The backbone's thickness and the height were set at 2mm and 40mm, respectively. As bending stresses were higher at the manipulator's base, the backbone's thickness of Module 2 was increased to 4mm. Each yaw module was also installed with spacer disks of 50mm outer diameter and with a distance of 50mm between adjacent spacer disks.

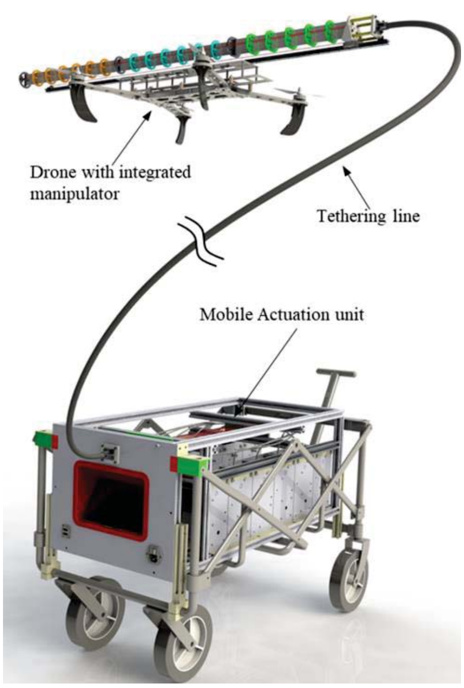

Fig. 2 Cable-Driven Continuum Manipulators with Tethering Lines system

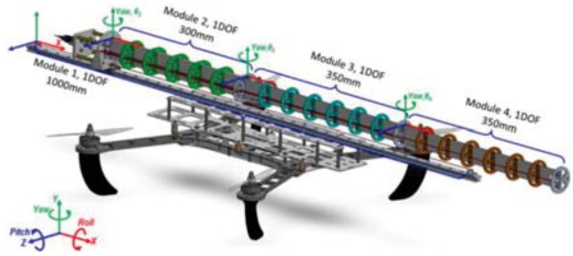

Fig. 1 Kinematic diagram of the cable-driven continuum manipulator

3. Kinematics Model

For this cable-driven continuum manipulator, the modified D-H method with constant curvature assumption [2] was adopted to establish its forward kinematics model. As seen from Fig. 3, there were a total of 20 spacer disks with a distance of 50 mm between them. Modules 2, 3 and 4 were considered as joints with joint angle θ_2, θ_3 and θ_4, respectively. The backbone ideally followed a constant curvature assumption. In case the actual backbone curvature exhibited discrepancy, then the other spacer disks would be considered in the D-H parameters as sub-joints that could be configured by incorporating compensation factors for the joint angles. The D-H parameters were established according to kinematic diagram in Fig. 3, and as listed in Table 1. The number in row 2, 2:2:12 meant that a set of joint number started at 2, and ended at 12, with each joint number separated by 2. This numbering convention was also applied to the next rows. X in Table 1 represented the shortest distance from start to end of the backbone, which was the joint angle dependent with the following relationship:

$$|X| = \frac{s}{\theta}\sin\theta \tag{1}$$

The homogenous transformation matrix between two successive frames followed those in [3] and re-written as follows:

$$ {}_{n+1}^{\;\;n}T = \begin{bmatrix} C\theta_{n+1} & -S\theta_{n+1}C\alpha_{n+1} & S\theta_{n+1}S\alpha_{n+1} & a_{n+1}C\theta_{n+1} \\ S\theta_{n+1} & C\theta_{n+1}C\alpha_{n+1} & -C\theta_{n+1}S\alpha_{n+1} & a_{n+1}S\theta_{n+1} \\ 0 & S\alpha_{n+1} & S\alpha_{n+1} & d_{n+1} \\ 0 & 0 & 0 & 1 \end{bmatrix} \tag{2}$$

where the notation C and S refer to sine and cosine, respectively.

In order to demonstrate the viability of the proposed manipulator design and the proposed kinematics model, the cable-driven continuum manipulator was simulated to reach back of the pot bearing. Due to space constraints, it required 6 steps in order to reach the back of the pot bearing. A combination of linear motion and joint angles was employed to perform this task (see Table 2 for details of each step). A Matlab® code generated the kinematic model parameters according to the developed plant model and simulated. Fig. 4 showcased the plotted results of every step, It was seen that the end-effector followed the pot-bearing outer diameter without being in contact (otherwise, this would mean a collision during operations) with either the pot bearing or the crevice wall.

4. Simulation Studies

Finite element analysis (FEA) was also conducted to calculate deformation and stress distributions of the manipulator during operation. A 3-D finite element model of the proposed continuum manipulator was developed, and static analysis was performed in Solidworks®. The applied boundary conditions in static analysis were fixed constraint at the base and with gravity applied to the whole manipulator. Deformation and stress distribution plot of the manipulator during Step 1 (i.e., initial position) was plotted (see **Error! Reference source not found.**(a) and 5(b) respectively). A maximum deformation of 7.6mm was observed at the manipulator tooltip and the maximum stress was observed at the start of Module 3 (i.e., von Misses stress of 3.5MPa), which was far below the material's Yield strength 63MPa.

Deformation and stress distribution plot of the manipulator during Step 6 (i.e., tooltip reaching the back of the pot bearing housing) was

Table 1 D-H Parameters

i		*d*	*a*	
1	0	d1	-90	0
2:2:12	n	0	0	90
3:2:13	0	X2	0	90
14:2:26	n3	0	0	-90
15:2:27	0	X3	0	90
28:2:40	n4	0	0	-90
29:2:41	0	X4	0	90

Table 2 Step by step of axial translation of Module 1 and yaw angles of Modules 2, 3 and 4 to reach back of the pot bearing

Step	d_1	θ_2	θ_3	θ_4
1	0	0	0	0
2	170	0	0	-55
3	280	0	-28	0
4	520	0	-55	74
5	615	-29	0	74
6	850	-58	72	74

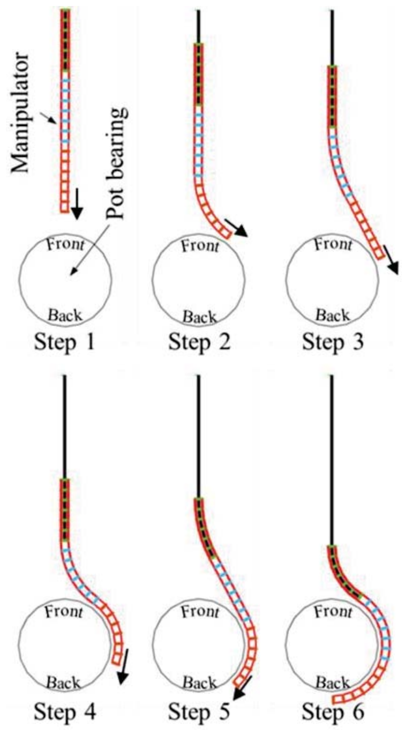

Fig. 2 Top view of the six steps in order to reach the back of the pot bearing

also plotted (see **Error! Reference source not found.**(a) and 6(b) respectively). The maximum deformation of 165mm was observed at the tip and the maximum stress was observed at the start of Module 3 (i.e., von Misses stress of 9.18MPa), which was still below the material's Yield strength of 63MPa. While the material deformation was still within elastic range, the deflection of the tooltip was quite significant. This large deflection was due to manipulator's backbone profile rigidity, where in Step 6, the manipulator's center of gravity was shifted to the side and causing a torsional effect. The backbone curvature in Step 6 would be considered the worst-case scenario as the manipulator is only required to reach the back of the pot bearing housing, and not expected to curl around and return to the front of the pot bearing housing.

5. Prototype Development and Experimental Validation

In order to validate the manipulator's kinematic model, the cable-driven continuum manipulator prototype was fabricated and tested. The material of the spacer disks, other than at the end of the Modules 2-4, was selected to be Delrin® because this material exhibited low frictional coefficient, and would minimize the frictional effects of the actuation cables running through them. The spacer disks, especially at the end of Modules 2, 3 and 4 would experience higher bending stresses because the actuation cables terminated at these disks. Therefore, Aluminum was selected as the material for these spacers, due to its higher yield strength, as compared to Delrin®. The total weight of the manipulator including the linear guide rail and carriage resulted to 645 grams. Lightweight design is always preferred, especially when combining with an aerial drone.

The fabricated prototype was then connected to the tethering line and the actuation unit controlled by kinematics models to perform a series of motions shown in Fig. 4. The pose of the manipulator was recorded during operation from Steps 1 to 6, as seen in **Error! Reference source not found.**. It was seen that the horizontal profile followed the profile shown in Fig. 4. However, due to the effects of gravity and low torsional rigidity of the backbone, the manipulator deflected downward, with the largest vertical deflection of 165mm occurring at Step 6. This was consistent with the simulation results (with approx. 95% accuracy).

6. Conclusion

The design of the cable-driven continuum manipulator, which was inspired by the flexible ruler, offered high bending stiffness in the vertical direction to minimize downward deflection of the manipulator, with low bending stiffness in the horizontal direction. A kinematics model based on the modified D-H method, with a constant curvature compensation factor was developed and verified with experimental trials. While the proposed design performed well for small curvatures, future work will include enhancements to the backbone design for greater rigidity when having larger curvatures.

ACKNOWLEDGEMENT

This work was supported by the 'Intelligent Ground-Aerial Robots for Closed Quarters Interactive Operations' project (Grant ID: 1922500056), under A*STAR's 'National Robotics Programme'.

REFERENCES

1. QingHui Yuan, Jae Lew, Damrongrit Piyabongkarn, "Motion Control of an Aerial Work Platform," 2009 American Control Conference, pp. 2873-2878, 2009.
2. Hannan, M.W. and Walker, I.D., "Kinematics and the Implementation of an Elephant's Trunk Manipulator and Other Continuum Style Robots" J. Robotic System, Vol.20, No.2 pp. 45-63, 2003.

3. Niku, Saeed B., “Introduction to Robotics: Analysis, Control, Applications”, Hoboken, N.J: Wiley, 2011.